Attitude Dynamics of a Tethered CubeSat-Inflatable System in Low Earth Orbit

AE 8900 MS Special Problems Report
Space Systems Design Lab (SSDL)
Guggenheim School of Aerospace Engineering
Georgia Institute of Technology
Atlanta, GA

Author:
Alexander J. Boisvert

Advisor:
Prof. Brian C. Gunter

April 26, 2018

Attitude Dynamics of a Tethered CubeSat-Inflatable System in Low Earth Orbit

Alexander J. Boisvert,[1] and Brian C. Gunter[2]
Georgia Institute of Technology, Atlanta, GA, 30313, USA

This paper analyzes the attitude dynamics of an inflatable tetrahedron tethered to a 3U CubeSat via a 10 meter tether. In previously flown space tether missions the primary moment on the system being considered is the gravity gradient torque. In this analysis, however, the large area to mass ratio of the target increases the impact of drag and solar radiation moments so they are also examined. The dynamics of the deployed system was analyzed using the 42 spacecraft simulator, an open source simulation software developed by NASA Goddard. Both single and 10 element tethers were analyzed at altitudes ranging from 300 kilometers to 600 kilometers. They system showed the potential to develop unstable oscillations when uncontrolled but an active damping control scheme shows potential for maintaining the stability of the system. The deployment of the tether is analyzed as a damped spring system in SIMULINK. The deployment is analyzed for three deployment speeds and three potential damping ratios. The impact of this analysis on the requirements for the attitude determination and control subsystem are also considered.

I. Nomenclature

F	=	force vector
dF	=	differential force vector
μ	=	standard gravitational parameter
r	=	inertial frame position magnitude
$\hat{r}$	=	inertial position unit vector
I_{xx}	=	x-axis principle moment of inertia
I_{yy}	=	y-axis principle moment of inertia
I_{zz}	=	z-axis principle moment of inertia
M	=	moment vector
dm	=	differential mass
dr	=	inertial position vector to differential mass
ω	=	angular rate
$\dot{\omega}$	=	angular acceleration
l	=	distance from center of mass center of pressure
θ	=	deflection from local vertical
φ	=	deflection from velocity vector
$\emptyset$	=	solar flux at 1 AU
ϑ	=	solar incidence angle
c	=	speed of light
ρ	=	density
C_d	=	drag coefficient
V	=	inertial velocity vector
$\hat{V}$	=	inertial velocity unit vector
S	=	reference area
n	=	mean motion
q	=	reflectance factor

[1] Master's Student, Daniel Guggenheim School of Aerospace Engineering, Member AIAA
[2] Assistant Professor, Daniel Guggenheim School of Aerospace Engineering, Senior Member AIAA

L = Lagrangian
T = kinetic energy
U = potential energy
k = spring constant
A = cross-sectional area

Subscripts

x = x axis component
y = y axis component
z = z axis component
g = due to gravitational effects
d = due to drag effects
SRP = due to solar radiation pressure
cp = center of pressure

II. Introduction

The analysis in this report focuses on the Tethering And Ranging mission of the Georgia Institute of Technology (TARGIT). The primary goal of this mission is to demonstrate the functionality of a compact in-space LiDAR system that could be used for topographical mapping in planetary missions. The system is a 3U CubeSat that deploys an inflatable tetrahedral target, with an edge length of one meter, that will be imaged using the LiDAR instrument. The anticipated mass of the CubeSat is 4.5 kilograms and that of the target is 0.508 kilograms. The system will have full 3-axis attitude control using reaction wheels supplemented with torque rods. An optical camera will be used to track the target's position initially and be used to verify the deployment of the target.

It was noted early on that the high area to mass ratio of the target would cause it to drift away from the CubeSat in a matter of hours. The target has an area to mass ration of 0.85 square meters per kilogram to the CubeSats 0.0022 square meters per kilogram when considering the1U side or 0.022 square meters per kilogram when considering a side profile with its solar panels fully deployed. It was deemed that this limited window to image the target incurred too

much risk to the mission. To mitigate this risk and drastically extend the duration of the science mission it was decided to initially tether the target to the CubeSat and later cut the tether and image the target as it drifts away.

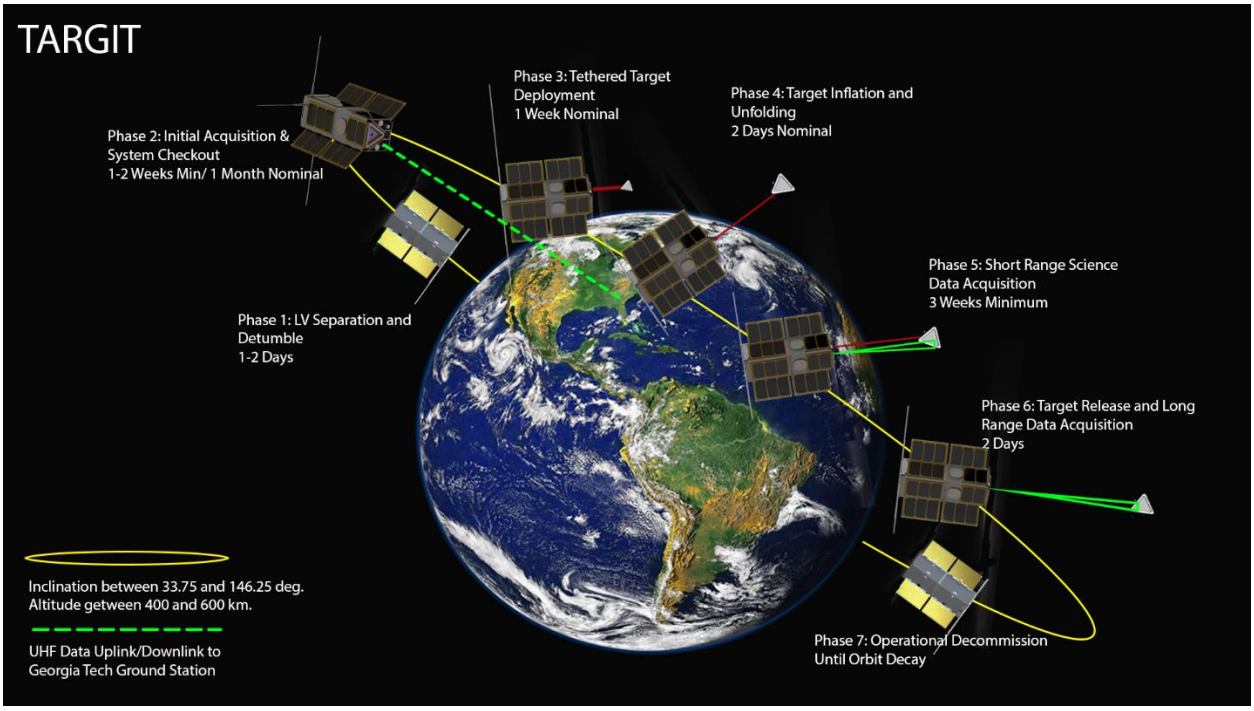

Figure 1: TARGIT Mission Operational Overview

The inclusion of the tether brings into question about the attitude dynamics of the system which in turn impact the design of several of the mission's subsystems. The primary motivation of this analysis is to aid in the design process of the CubeSat specifically the required pointing accuracy of the system, reaction wheel requirements, optical camera field of view, and the orientation of the system for use in communications and recharging. This report will analyze the system to determine its level of stability, stable orientation, and deployment risks. The system is analyzed for a range of low Earth orbits from 300 kilometers to 600 kilometers in 50 kilometers increments. Understanding the dynamics that govern this system would prove a benefit to future mission that may wish to use a similar architecture. This is particularly applicable to the use of inflatables as drag devices in low Earth orbit.

A. Previous Tethered Satellite Missions

Tethered satellite systems have been an active area of research for several decades and have been flown on several missions. They have been considered for several applications including: formation flying, propulsion, attitude control, and more recently for debris removal. The first tethered system to be flown in space was during the Gemini 11 mission in 1966 which used a 30 meter tether to connect the Gemini capsule with the Agena Target Vehicle to investigate gravity gradient stabilization and the generation of artificial gravity in space. The spacecraft rendezvoused in low earth orbit with a periapsis at 278 kilometers and apoapsis at 304 km. There was difficulty in establishing a passively stable gravity gradient orientation but the system was stabilized rotationally and was able to generate a small amount of artificial gravity. [1]

The next set of space tether missions was a pair of experiments conducted from the space shuttle, TSS-1 and TSS-1R. These missions relied on conducting tethers of approximately 20 kilometers in length to conduct plasma physics data and once again test the concept of gravity gradient stabilization. During TSS-1 the tether became stuck after reaching a length of 256 meter and the mission was unable to be completed. TSS-1R was the follow-on mission to TSS-1 and was also unsuccessful. Its tether broke after extending 19.7 kilometers but it was still able to collect some of its data. Another mission, designated TSS-2 was proposed but it was never selected. This marked the end of manned space tether missions. [1]

Following the manned missions NASA launched a trio of tethered satellite missions using the Small Expendable Deployer System (SEDS) in 1993 and 1994. The missions were called SEDS-1, SEDS-2, and the Plasma Motor Generator (PMG). SEDS-1 and SEDS-2 deployed an end mass of 26 kilograms attached to a 20 kilometer tether. The objective of the SEDS-1 mission was to demonstrate the ability of the SEDS platform to successfully deploy a 20 kilometers tether and to study the reentry of the end mass after cutting the tether. The mission was successful and the tether was cut after completing one orbit. SEDS-2 investigated the use of a closed loop control system to limit the deployment speed of the end mass to deploy the system along the local vertical while minimizing any librations in the system. The system deployed successfully with a libration of only 4 degrees and the control loop limited the final deployment rate to only 2 centimeters per second compared to SEDS-1 final speed of 7 meters per second. The mission was cut short, however, due to the tether breaking prematurely. This is suspected to have been caused by an impact from debris or a micrometeoroid. The PMG mission was this first in space demonstration of utilizing the electrodynamic properties of a 500 meter conducting tether for providing power and propulsion. The science phase of the mission lasted seven hours when the batteries died and successfully demonstrated both capabilities. [1]

The United States Navy also launched two tethered satellite missions the Tether Physics and Survivability Experiment (TiPS) and the Advanced Tether Experiment (ATEx). The goal of TiPS was to test the long-term survivability of a 4 kilometers tether in low Earth orbit where it survived for 10 years before the tether broke. The ATEx mission attempted to test active tether control and stability. Unfortunately, the tether was severed by the automatic safety system of the satellite after only deploying 22 meters of tether. [1]

In addition to the satellites built by government agencies there have been several university built tethered satellite missions. The Young Engineers' Satellites 1 and 2 (YES and YES2) were developed as a collaboration between the European Space Agency and university students. Both of these missions attempted to deploy tethered satellite systems. YES did not succeed in achieving its planned orbit so the system was not deployed. YES2 suffered a communications failure but telemetry suggests that the system successfully deployed its 35 kilometer tether to place its payload on a reentry trajectory as planned. [2] In addition to these missions two tethered satellite missions developed by Kagawa University in Japan have flown. These were the Space Tethered Autonomous Robotic Satellites (STARS and STARS-II). STARS planned to deploy a 5 meter tether but the deployment failed after only deploying several centimeters. The STARS-II mission deployed a 300 meter electrodynamic tether. The deployment of the tether could not be confirmed but the rapid deorbit of the system suggests that it was successful. [3]

There is an upcoming tethered CubeSat mission that plans to use a tether the same length of that on TARGIT. The mission is known as the Miniature Tether Electrodynamics Experiment (MiDEE) it is being developed by the University of Michigan and is scheduled to launch in late 2018. If successful it will be the first fully successful tethered CubeSat mission flown thus far. MiDEE is using the same 3U form factor as TARGIT but the end mass on its tether is very different from that of TARGIT. MiDEE uses a small, compact sub-satellite as an end mass to help pass current through the tether for electrodynamic propulsion. Given the small form factor of the sub-satellite drag is not nearly as critical of a factor as it is on the TARGIT mission. [7&8]

The TARGIT mission is a departure from more traditional tethered satellite system in two significant aspects the first of which is the length of the tether. Previously flown tether missions have utilized tethers that are hundreds of meters to several kilometers in length, with the exception of the STARS mission which failed to deploy, but the tether proposed in the TARGIT mission is only 10 meters in length. This limits the impact of gravity gradient torques which attempt to stabilize the system along the local vertical. The second departure from space tether mission norms is the end mass. The end masses in the previously mentioned missions have all been fully functional satellites or an electronics package so the area to mass ratios have been small. The inflatable magnifies the impact of drag and solar radiation pressure. These effects will be examined in detail in the following sections.

III. Driving Torques

In previous examinations of tethered satellite systems, the analysis has focused almost exclusively on the impact of gravity gradient torques on the system. This can be justified when considering most satellite systems especially outside of low Earth orbit. This is not the case, however, for the TARGIT mission. CubeSat missions allow for experiments to be conducted in space at a greatly reduced cost making them ideal for universities and small companies. When deployed the inflatable target will increase the area to mass ratio of the system by an order of magnitude. This increased area will drive up the impact of both drag and solar radiation torques on the system making them no longer negligible. The magnitudes of these torques as a function of altitude can be seen in the figure below. The figure was generated using orientations that would maximize each of the moments. This is aligned along the velocity vector for

the solar radiation moment, aligned along the local vertical for the drag moment, and 45 degrees between the velocity vector and the local vertical for the gravity gradient moment. The reference area of the target was assumed to be 0.43 square meters to reflect the area of one side of the tetrahedron. The area of the CubeSat was 0.01 square meters when ram aligned and 0.09 square meters, accounted for deployed solar panels, when aligned with the local vertical.

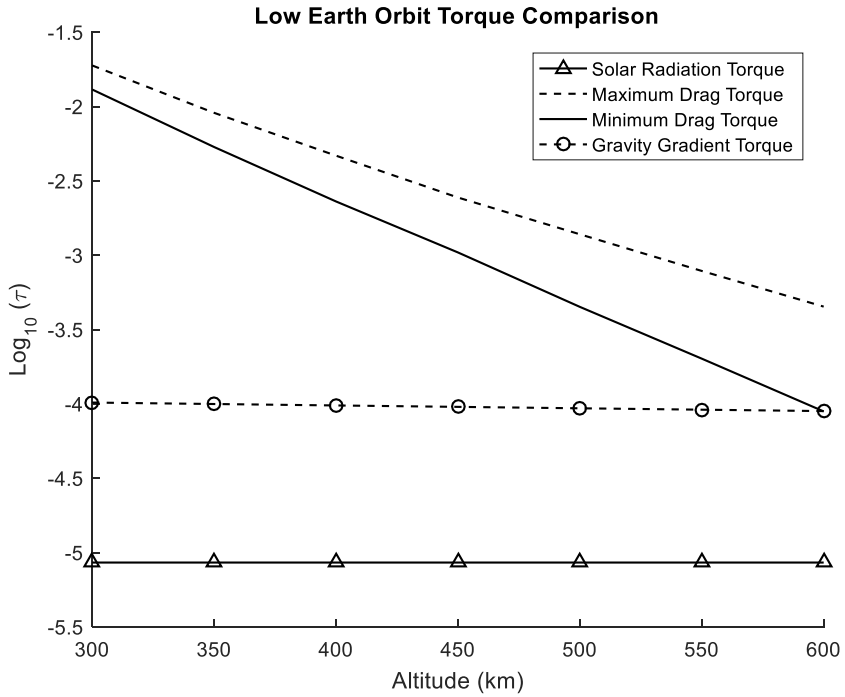

Figure 2: Driving Torques in Low Earth Orbit

It can be seen from the figure that while the gravity gradient and solar radiation torques remain consistent with altitude the torque due to drag decreases greatly. The maximum and minimum drag torque lines correspond to the diurnal variations expected at each altitude. These values were generated using the NRLMSISE-00 atmosphere model. At lower altitudes it is clear that the drag torques are dominant but at around 500 kilometers the gravity gradient torques begin to become comparable. The solar radiation pressure effects only begin to become significant at the highest altitudes being considered and even then they are not as dominant as the gravity gradient and drag effects. It is also important to note that the solar radiation pressure is not a factor while the spacecraft is in eclipse. The similarity in the magnitudes of these torques greatly impacts that attitude dynamics of the system. These effects will be more thoroughly examined in the section below.

B. Gravity Gradient Effects

The force of gravity between two, point masses is calculated via the following equation:

$$\vec{F}_g = -\mu \frac{\hat{r}}{r^2} \quad (1)$$

This simplification is useful for the prediction of the trajectory of the system but cannot describe the small changes in the gravitational force along a rigid body. To accomplish this a differential gravitational force equation must be used. This equation can then be integrated across the mass of the body.

$$d\vec{F}_g = -\mu \frac{\hat{r}}{r^2} dm \quad (2)$$

$$\vec{M}_g = \int_m (d\vec{r} \times d\vec{F}_g)\, dm \quad (3)$$

When integrated the moment equation yields the following: [6]

$$M_{g,x} = \frac{3\mu r_z r_y}{r^5}(I_{zz} - I_{yy}) \quad (4)$$

$$M_{g,y} = \frac{3\mu r_x r_z}{r^5}(I_{xx} - I_{zz}) \quad (5)$$

$$M_{g,z} = \frac{3\mu r_y r_x}{r^5}(I_{yy} - I_{xx}) \quad (6)$$

Where $\frac{r_x}{r}, \frac{r_y}{r}$, and $\frac{r_z}{r}$ are the direction cosines of the vector to the center of mass. To allow for a body fixed rotating reference frame as the satellite orbits the Earth, Euler's equations of motion must be used.

$$I_{xx}\dot{\omega}_x + (I_{zz} - I_{yy})\omega_y\omega_z = \frac{3\mu r_z r_y}{r^5}(I_{zz} - I_{yy}) \quad (7)$$

$$I_{yy}\dot{\omega}_y + (I_{xx} - I_{zz})\omega_x\omega_z = \frac{3\mu r_x r_z}{r^5}(I_{xx} - I_{zz}) \quad (8)$$

$$I_{zz}\dot{\omega}_z + (I_{yy} - I_{xx})\omega_y\omega_x = \frac{3\mu r_y r_x}{r^5}(I_{yy} - I_{xx}) \quad (9)$$

The gravity gradient torque has equilibrium positions: the axis of minimum inertia aligned vertically or horizontally. Of the two equilibrium orientations only the vertical case is stable. In the presence of other perturbing torques, such as drag and solar radiation pressure, this stable orientation shifts. [9] These stability orientations for the TARGIT system can be seen in Table 2. For the stability considerations just mentioned perturbations about the vertical axis are of the most interest and it will be the axis considered for the remainder of this analysis. This also allows for the dynamics of the system to be drastically simplified. If the system is restricted to only rotate about in the orbital plane, normal to the x-axis and the system follows a circular orbit the perturbation angle of the x axis and the local vertical "θ" is given by the following:

$$M_{g,x} = \frac{3\mu \sin(2\theta)}{2r^3}(I_{zz} - I_{yy}) \quad (10)$$

If only small angle perturbations are considered the system can be modeled as a simple harmonic oscillator with an angular frequency of:

$$\omega = \sqrt{\frac{3\mu}{r^3}\frac{(I_{zz} - I_{yy})}{I_{xx}}} = n\sqrt{3\frac{(I_{zz} - I_{yy})}{I_{xx}}} \quad (11)$$

Where n is the mean motion of the system. It is important to note that the above equation relies on the small angle approximation to linearize rotational dynamics and is not accurate for large angular perturbations. To more accurately describe how the system behaves at higher angular perturbations simulations can be used.

C. Drag Effects

The drag force experienced by the satellite is given by:

$$\vec{F}_D = \frac{1}{2}\rho(\vec{V}\cdot\vec{V})SC_d\hat{V} \quad (12)$$

The moment generated by drag for each body is given by the following equation:

$$\vec{M}_D = \vec{r}_{cp} \times \vec{F}_D \quad (13)$$

To simplify the drag moment equation, it is assumed once again that the system only rotates about the orbital plane, normal to the x-axis and follows a circular orbit.

$$M_{D,x} = \frac{1}{2}\rho V^2 SC_d l \sin(\varphi) \quad (14)$$

In a drag dominant case the system will be stable when oriented along the velocity vector and φ is the deflection from this orientation. This will be stable if the low drag body is leading and unstable if the high drag body is leading. Due to the CubeSat having a much smaller drag area than the target and shorter distance to the center of mass the moment generated by the body of the CubeSat is ignored. If small angle perturbations are assumed as were for the gravity gradient analysis the system can once again be modeled as a harmonic oscillator with a frequency of:

$$\omega = \sqrt{\frac{\rho V^2 SC_d l}{2\, I_{xx}}} = nr\sqrt{\frac{\rho SC_d l}{2\, I_{xx}}} \quad (15)$$

The above equations assume a constant atmospheric density at a given orbital altitude. For most satellite applications, even for many tethered systems, this is adequate assumption as they generally have relatively low drag area to mass ratios or operate above low Earth orbit. For this case, however, drag torques have a significant impact on the attitude dynamics of the system so density variations must be considered. The 42 Simulation Framework uses the NRLMSISE-00 atmospheric model so it will be used to examine how the density of the atmosphere varies. This model was released in 2000 by the US Naval Research Laboratory and was developed empirically primarily using mass spectrometer and incoherent scatter radar data. It considers a variety of inputs including latitude, longitude, altitude, time of day, solar flux, and magnetic flux. The following figure shows how the atmospheric density varies along a 400 kilometer orbit. The starting date for the density profile in the figure is September 1, 2019 in accordance with the anticipated mission timeline.

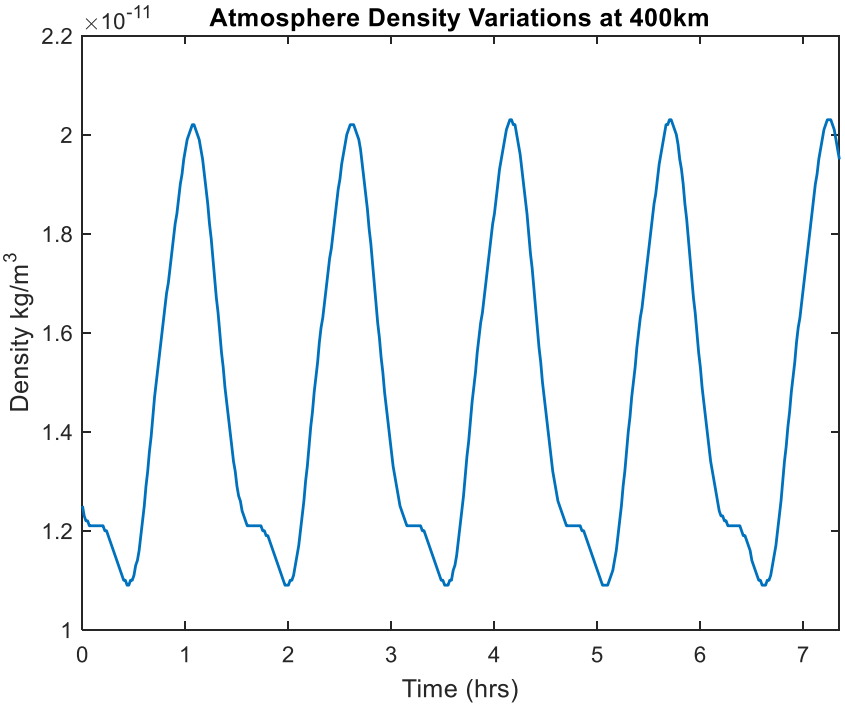

Figure 3: Diurnal Atmosphere Density Variations

The density of the atmosphere varies in a roughly sinusoidal manner whose maximum indicates the Sun being directly over the spacecraft. The density oscillates with the same frequency as the mean motion of the spacecraft. If this density variation is included into the drag moment equation it becomes difficult to develop an analytical solution to determine how system evolves with time. The period of the small oscillations due to drag and gravity gradient effects can be seen in the following table.

Table 1: System Oscillations

	Oscillations Per Orbit		
Altitude	Gravity Gradient	Low Drag	High Drag
300km	1.66	13.27	15.98
350km	1.66	8.59	11.20
400km	1.66	5.70	8.13
450km	1.66	3.88	5.94
500km	1.66	2.58	4.52
550km	1.66	1.74	3.44
600km	1.66	1.17	2.64

D. Solar Radiation Pressure

This effect describes the pressure experienced by the spacecraft due to the radiation emitted by the Sun. It varies along with the solar cycle which is approximately 11 years. The variations, however, are small and can be seen in the figure below.

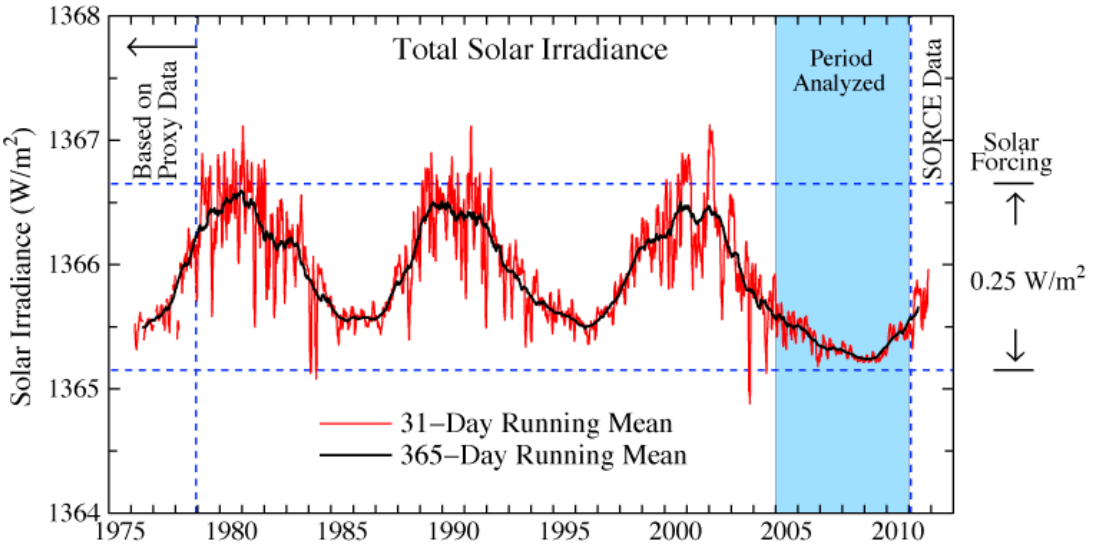

Figure 4: Solar Cycle Irradiance Variations[4]

The force it exerts on a spacecraft can be calculated by the following equation:

$$F_{SRP} = \frac{\emptyset}{c} S(1+q) \quad (16)$$

This can be translated into a moment using the equation:

$$M_{SRP} = \frac{\emptyset}{c} S(1+q) l \cos(\vartheta) \quad (17)$$

Where ∅ is the total solar flux at 1 astronomical unit which is approximately 1366 watts per meter squared and q is the reflectance of the material being considered. The reflectance can range from zero, if the material absorbs all of the energy, and one, if the material reflects all of the energy. For the purposes of this analysis the reflectance was assumed to be 0.85, approximately the value for aluminized Mylar [5]. The effects of solar radiation pressure on a spacecraft are generally minimal but due to the relatively large area of the target it must be considered. While even in the TARGIT missions case the moment it exerts is still an order of magnitude less than the gravity gradient and drag torques it is maximized when the spacecraft is in an orientation where the others are minimized. The total impact of these moments is examined in the following section.

E. Net Impact

The impacts of each of the moments on the satellite that have been discussed are heavily dependent on the attitude of the spacecraft and when all of the moments are added together no analytic solution for the attitude of the spacecraft can be determined. The magnitudes off the moments as a function of altitude can be seen in Figure 2 and it can be clearly seen that drag and gravity gradient torques are more dominant at all altitudes. It is also important to note that there is no effect from solar radiation pressure while the satellite is in eclipse. The density of the atmosphere also changes based on if the satellite is in eclipse. This diurnal effect decreases the drag on the spacecraft during eclipse and increases it when it is not. The following two figures show the day light, high drag, torques and the eclipse, low drag, torques.

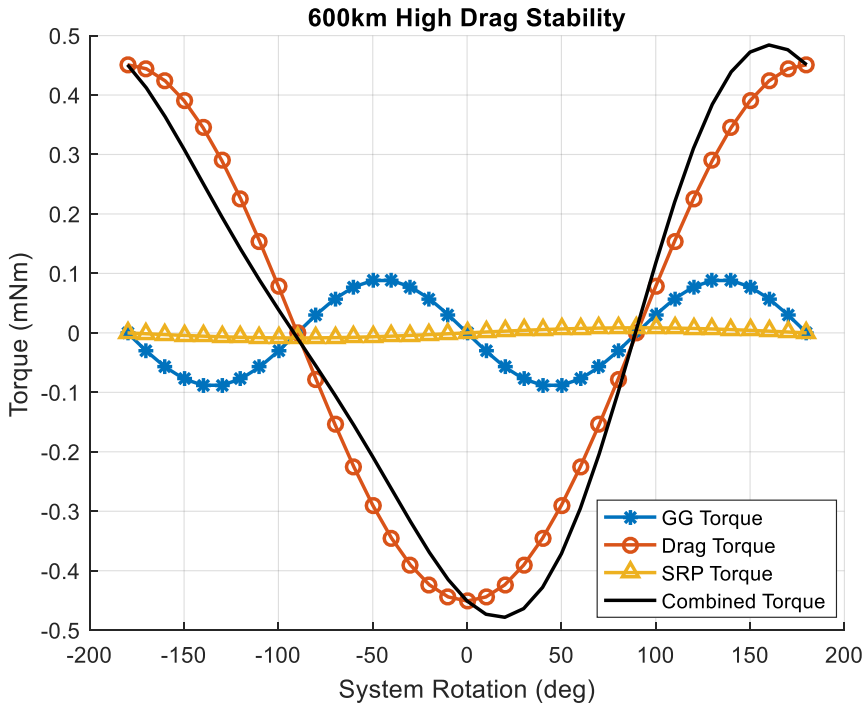

Figure 5: System Moments on Dayside

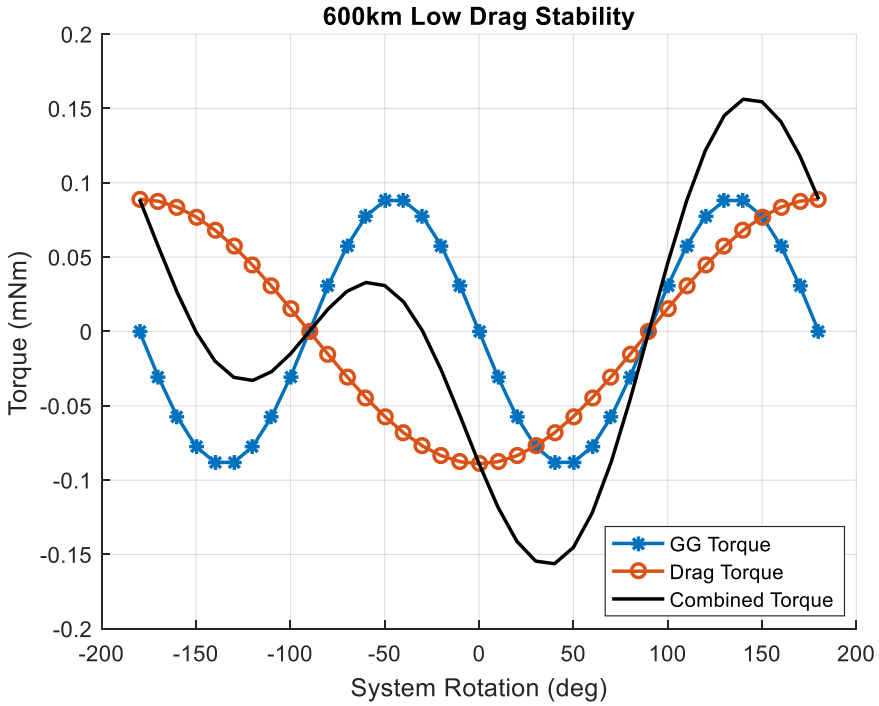

Figure 6: System Moments During Eclipse

The points where the plots cross zero on the y-axis are where all of the torques being considered cancel out and are orientations where the satellite is in an equilibrium position. Where the y axis is crossed with a positive slope the orientation is an unstable equilibrium and where it is crossed with a negative slope it is a stable equilibrium. Along the system rotation axis, the zero degree point is where the system is aligned along the local vertical and the -90 degree point is when the system is aligned with the velocity vector with the target trailing the CubeSat. Figures 5 and 6 show the moments at a 600 kilometer orbit. The stable equilibrium of the system at orbits ranging from 300 kilometers to 600 kilometers is presented in the table below. It is important to note that in Table 2 the zero degree point is when the system is aligned along the velocity vector with the target trailing.

Table 2: System Equilibrium Orientations

	Equilibrium Orientation (Deflection from Velocity Vector)		
Altitude	Low Drag	High Drag	High Drag with SRP
300 km	0^o	0^o	-0.03^o
350 km	0^o	0^o	-0.06^o
400 km	0^o	0^o	-0.11^o
450 km	0^o	0^o	-0.22^o
500 km	0^o	0^o	-0.42^o
550 km	0^o	0^o	-0.82^o
600 km	$+/- 60.17^o$	0^o	-1.8^o

It can be seen from Table 2 that for the majority of low Earth orbits being considered the system will be most stable oriented along the velocity vector. This is not the case, however, for the 600 kilometer orbit where the gravity gradient moment overpowers the drag moment when the satellite is in eclipse. It can be expected that the system in a 600 kilometers orbit will experience large oscillations due to this difference in equilibrium conditions. The other cases seem as though they would be fairly stable considering that drag is the dominant moment on the system both in and out of eclipse. The impact of solar radiation pressure in these cases, however, cannot be ignored. The solar radiation periodically exerts a force on the system which will make it begin to oscillate. This combined with the variations in drag can create oscillations that may increase in amplitude over time. It is also possible that these variations in the forces on the system could damp the oscillations out depending on the frequencies of the perturbing effects. Other damping factors on the system will be minimal as any drag due to lateral motion is negligible. To better understand how the system will behave simulations must be used.

IV. Fully Deployed Attitude Simulation

To analyze the fully deployed attitude dynamics of the system the simulation software 42 was used. 42 is an opensource simulation software written in C and developed by NASA Goddard[*]. This simulation software allowed for the rapid development of mission prototype simulations to determine the expected behavior of the system once it has been deployed. The software contains the NRLMSISE-00 atmosphere model which is the current standard being used in spacecraft simulations. It also includes a gravity model with up the 18th order spherical harmonics, an IGRF magnetic field model, and accurate solar radiation pressure modeling. It allows for the creation of both rigid and flexible multi-joint bodies as well as the simultaneous simulation of separate bodies to study the relative motion of two spacecraft. It isolates intra-body dynamics from its orbit propagation models which allows the simulation to run using larger time steps speeding up the simulation run time. The intra-body dynamics are calculated using Kane's Method and the orbit propagation can be selected from fixed, Euler-Hill, or Encke propagation methods. All propagation methods use a fixed time-step RK-4 integration scheme. 42 provides a rapid, open source, tool whose environmental and dynamics models have been verified by NASA. Without this software the analysis in this paper would have been impossible.

A. System Description

[*] 42 was downloaded from https://sourceforge.net/projects/fortytwospacecraftsimulation/, last accessed on 03/27/2018

The tethered satellite system is modeled in 42 in two different manner. The first being with a single element rigid tether and the second with a tether consisting of 10 rigid segments connected by freely rotating joints. The mass properties of the target, CubeSat, and tether being used in the simulation are presented in Table 3. The moments of inertia are calculated with respect to the center of mass of each body. The body frame definitions can be seen in the following figure.

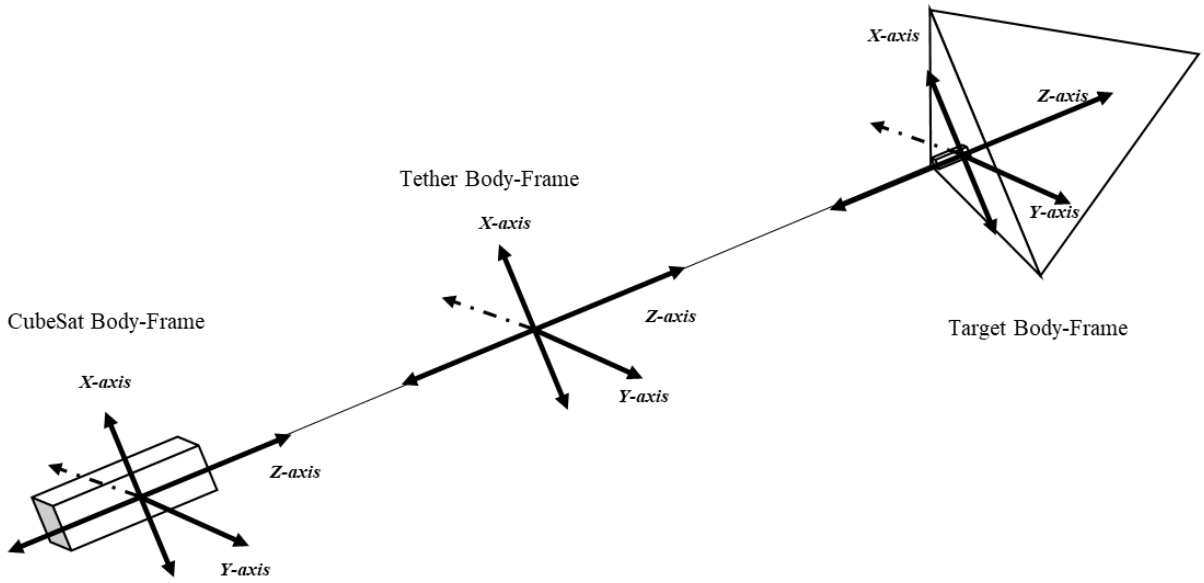

Figure 7: TARGIT System Body Frame Definitions

Figure 8: Starting Configuration for 42 Simulation, the pink axes correspond to the local coordinates where i_1 is the ram direction and i_3 is the local vertical

Table 3: Simulation System Mass Properties

	Satellite	*Target*	*Tether (10m length)*	*Tether (1m length)*
Mass (kg)	4.5	0.508	0.01	0.001
I_{xx} *(kg·m²)*	0.0375	0.0086	0.083	$8.3*10^{-5}$
I_{yy} *(kg·m²)*	0.0375	0.0086	0.083	$8.3*10^{-5}$
I_{zz} *(kg·m²)*	0.0075	0.0076	$1.25*10^{-9}$	$1.25*10^{-9}$

B. Single Element Tether Simulation

In a nominal state, where the tether remains fully extended under constant tension the system can be modeled as two bodies connected by a rigid tether. This system was simulated for two weeks to determine how a nominal, uncontrolled, system would behave in orbit. The system begins aligned along the velocity vector with an angular rate matching its mean motion so it would remain aligned with the velocity vector in the absence of any perturbing forces. The angular deflections from the velocity vector can be seen in the plots below.

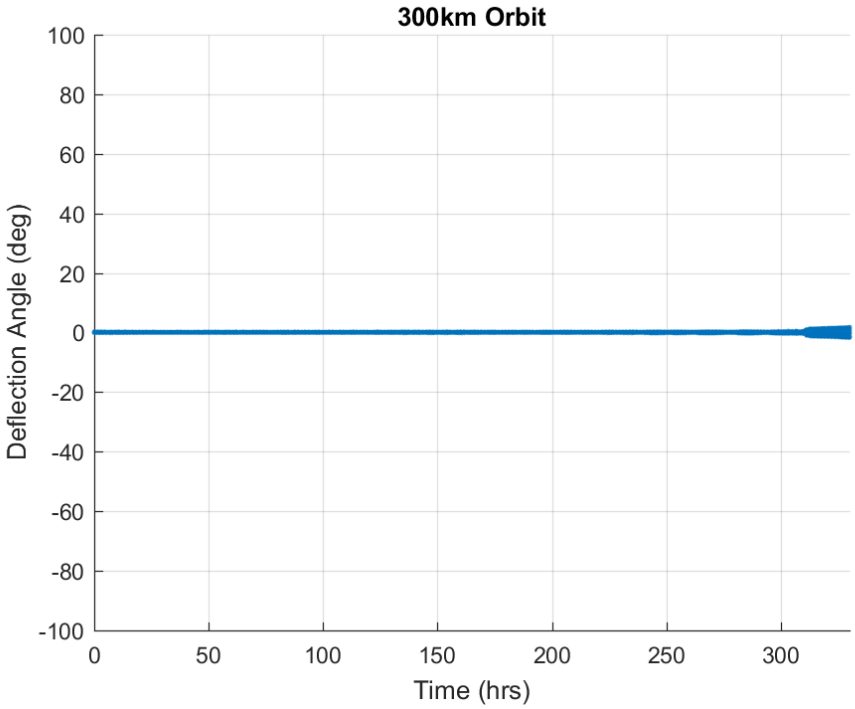

Figure 9: Deflection from Velocity Vector, 300km

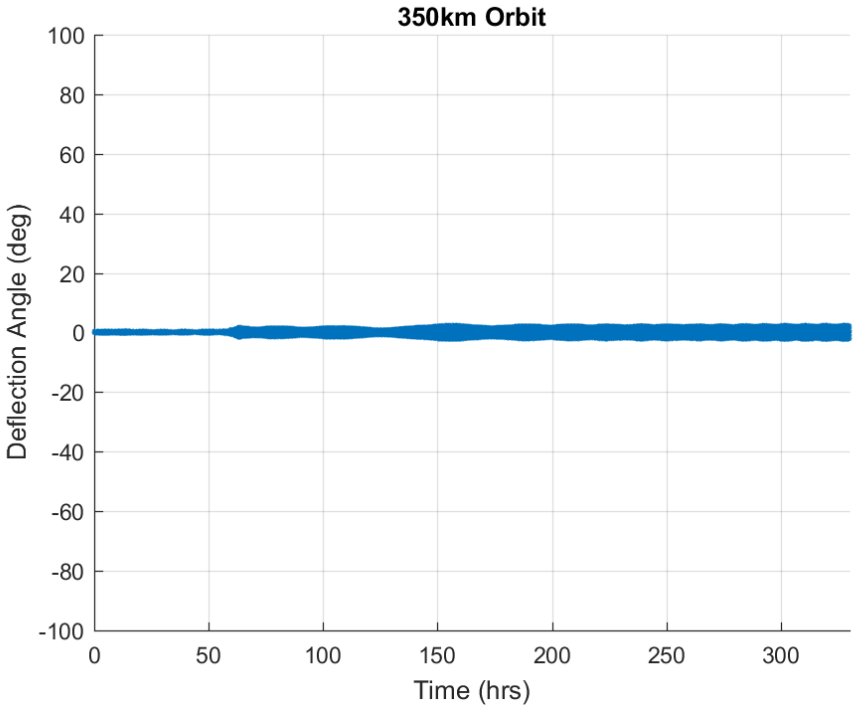

Figure 10: Deflection from Velocity Vector, 350km

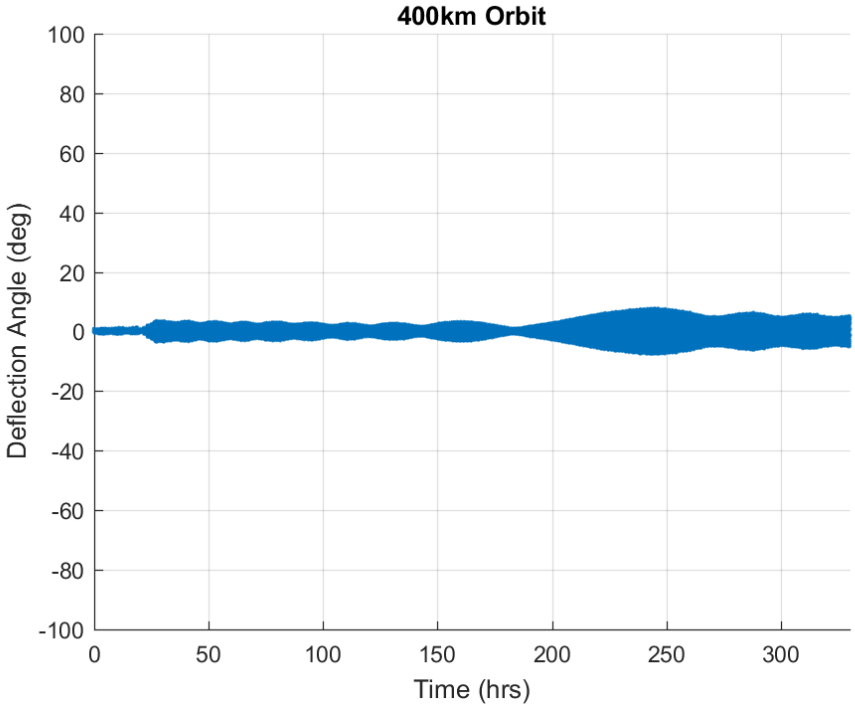

Figure 11: Deflection from Velocity Vector, 400km

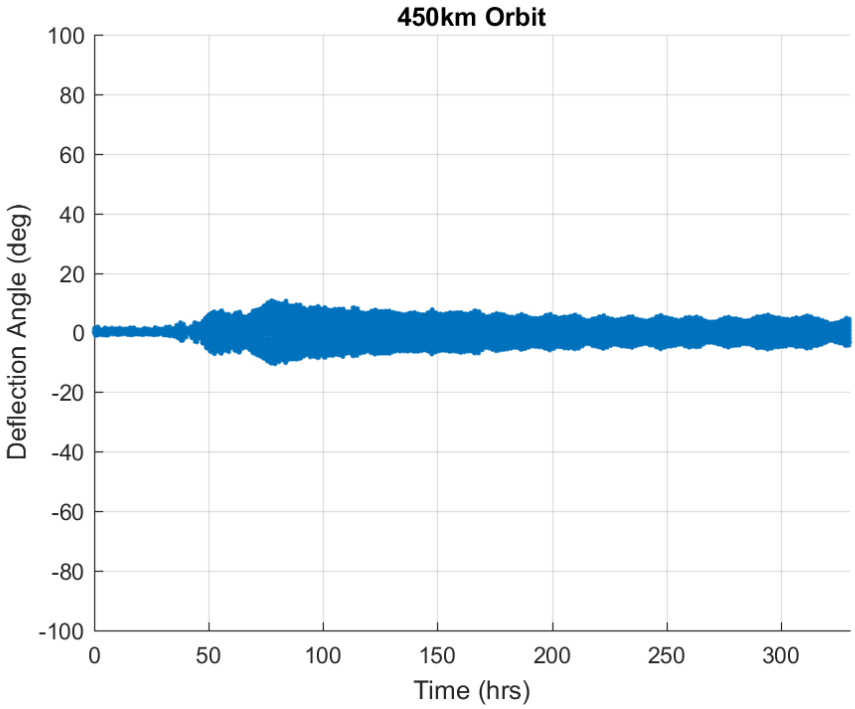

Figure 12: Deflection from Velocity Vector, 450km

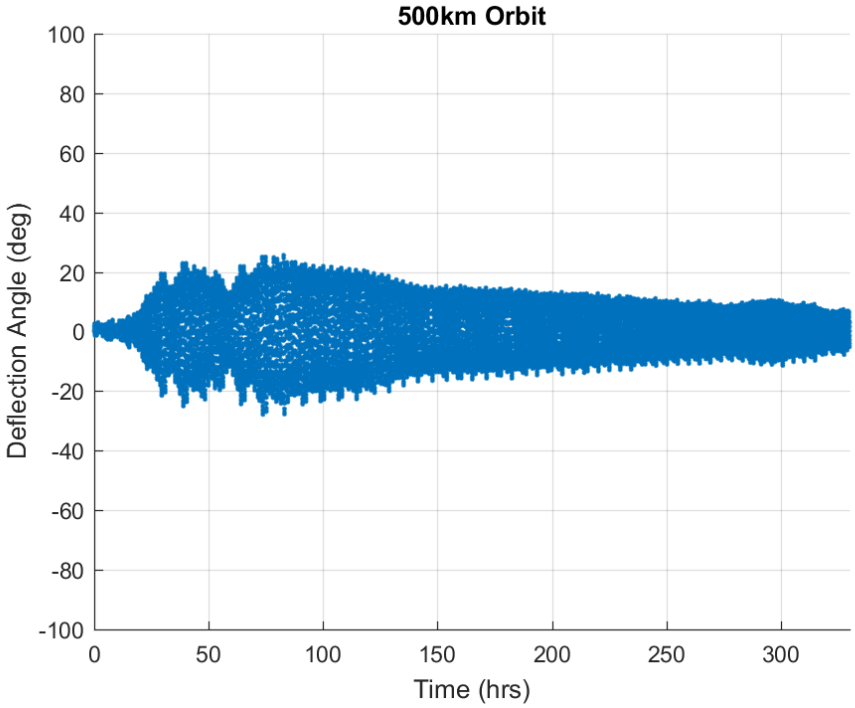

Figure 13: Deflection from Velocity Vector, 500km

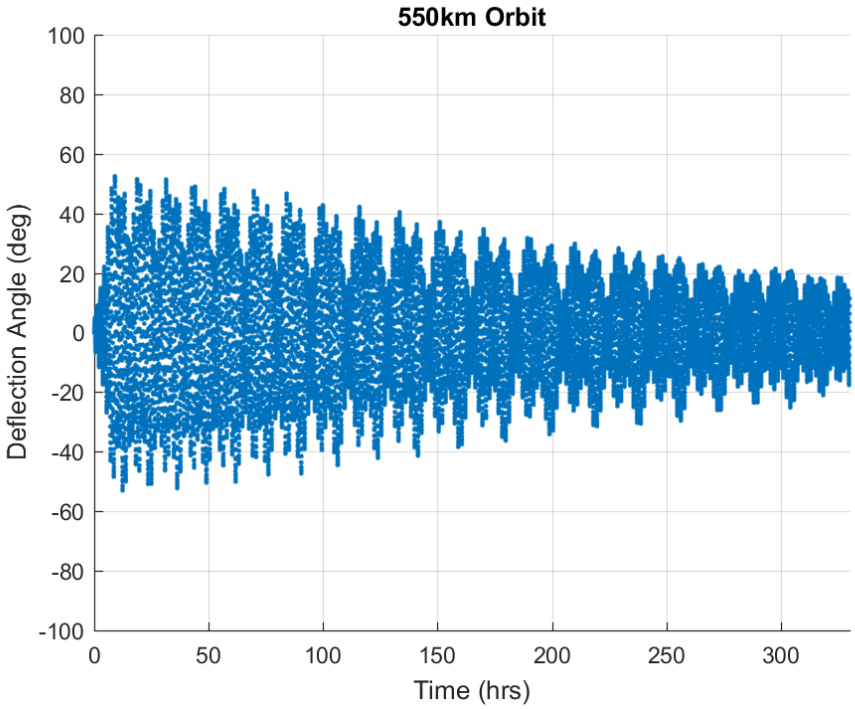

Figure 14: Deflection from Velocity Vector, 550km

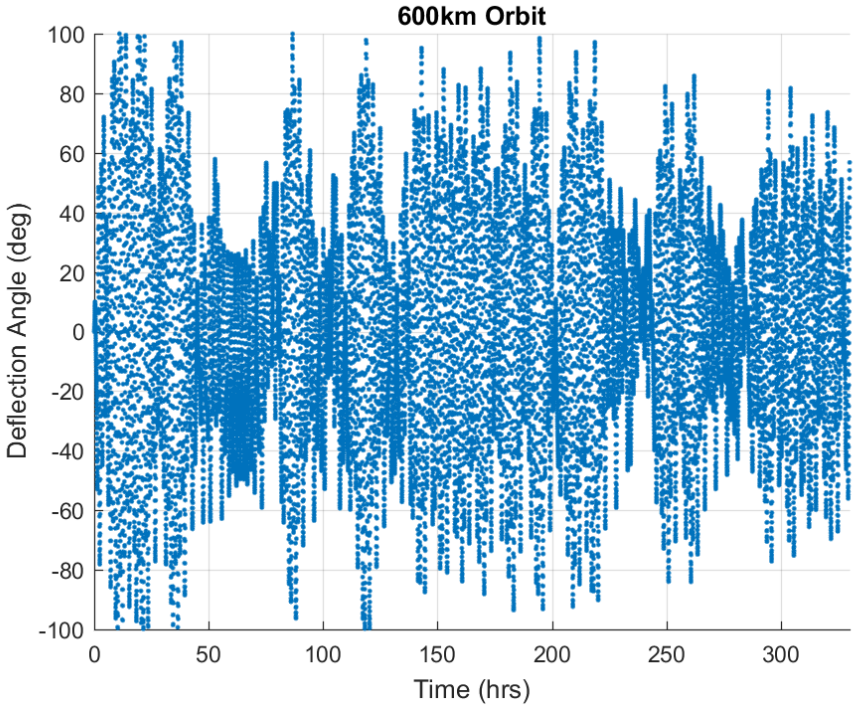

Figure 15: Deflection from Velocity Vector, 600km

It is clear from the figures above that, especially at higher altitudes, oscillations can develop and amplify. Due to the complex dynamics of the system its behavior is heavily dependent on its initial conditions. Since this oscillatory behavior occurs even in an ideal system a more refined simulation was deemed to be necessary. To combat the tendency for oscillations to develop a damping mechanism should be developed. An active damping method is introduced in the following section but a passive damping method could also be utilized.

C. Multi-Element Simulation

The simulation scenarios for the rigid tether simulations were repeated using a multi-element tether to more fully understand the intra-system dynamics that develop. A total of ten one-meter segments were used, each modeled as a rigid cylinder. It was discovered that like in the rigid cases oscillations would develop this increases the likelihood of oscillations developing in the tether leading to slack in the system. This ultimately causes the system to become unstable and risks the tether tangling around either the spacecraft or the target. This behavior caused instabilities to develop at all of the altitudes being considered. To mitigate this risk, it is necessary to develop a manner of damping oscillations in the system before they are able to amplify and cause instabilities. A basic active damping control was developed in which the CubeSat simply pointed opposite the direction that the target deflected from the velocity vector. The controller proved effective in reducing the oscillations in the system but a more refined method of damping would be required to ensure system stability. The deflection from the velocity vector in an uncontrolled and in a controlled case can be seen in the figures below.

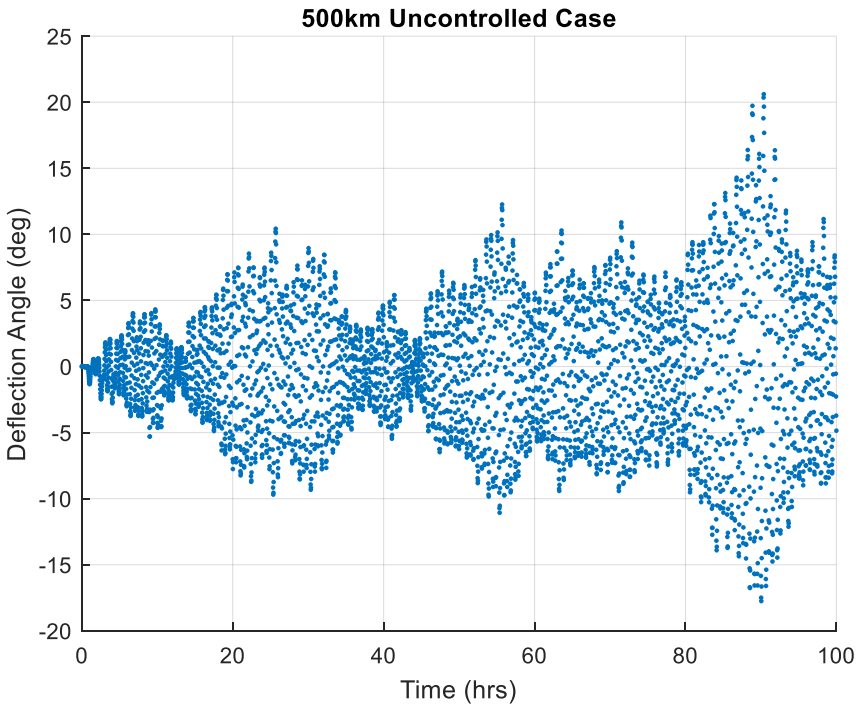

Figure 16: Deflection from Velocity Vector, 500km Uncontrolled System

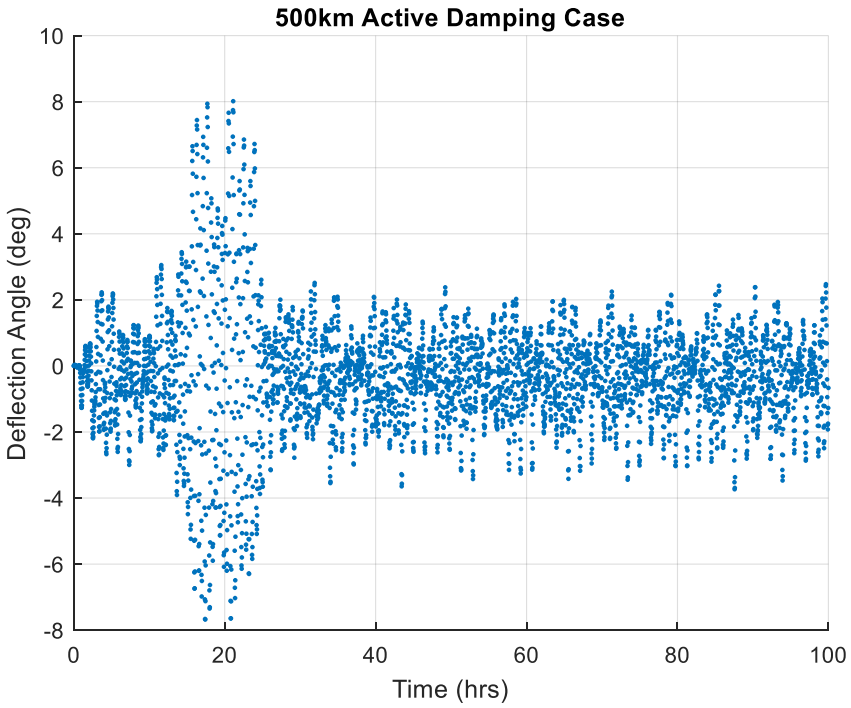

Figure 17: Deflection from Velocity Vector, 500km Active Damping Control

V. Deployment Simulation

The TARGIT mission intends to deploy the tether using a motor. This will give the system the ability to have a slow controlled release and to reel the tether back in if it is deemed necessary. If the tether is allowed to spool out too quickly there is a risk of the target bouncing back once it reaches full extension and either impacting the satellite or the tether becoming tangled. Both of these outcomes have the potential to result in mission failure so a maximum release speed must be determined. To analyze the tether deployment a model was created in SIMULINK. The tether is modeled as a stiff spring when it reaches full extension and ignored when it is not. The tether is assumed to be deployed at a constant speed. The equations governing the system are that of a two degree of freedom oscillatory system. This system can be solved using Lagrangian mechanics and the following energy equations.

$$\boldsymbol{L = T - U} \tag{18}$$

$$\boldsymbol{T = \frac{1}{2}(m_1 v_1^2 + m_2 v_2^2)} \tag{19}$$

$$\boldsymbol{U = \frac{1}{2} k (x_2 - x_1)^2} \tag{20}$$

The spring stiffness, k, is calculated from the Young's modulus of the material and the cross-sectional area of the tether via the following formula.

$$\boldsymbol{k = E * A} \tag{21}$$

The material being considered for the tether is Dyneema which is a polyethylene fiber. It has a Young's Modulus of 120 giga-pascals and the tether is assumed to be 0.3 millimeters in diameter. This results in a spring constant of 8,482 newtons per meter. In addition, the damping coefficient of the system must be considered. If there is no damping

the target and satellite will bounce back and forth on the tether continuously resulting in an unpredictable system. The damping coefficient must be determined experimentally so a range of damping coefficients is considered in this report. In an ideal case a damping coefficient would be chosen such that it makes the damping ratio unity. This is known as the critical damping coefficient and it would minimize the oscillations in the system. This would cause it to reach a steady state in the shortest period of time. The critical damping coefficient can be calculated using:

$$c_c = 2\sqrt{k\frac{(m_1+m_2)}{m_1 m_2}} \quad (22)$$

From this equation the ideal damping coefficient would be 274.58 newton-seconds per meter. The high value of which is due to the high Young's Modulus of Dyneema but a similar value would be expected for most non-elastic fibers. To achieve this damping coefficient the system would have to be able to disperse a large amount of energy. It is unlikely that the system will be able to perform in this manner so a range of lower damping coefficients are considered making the system under-damped. The driving factor when considering the release speed will be the expected orbit altitude with the higher altitudes have more stringent restrictions on deployment speed. This is due to the reduced drags at higher altitudes decreasing the natural separation time between satellite and target. The highest altitude being considered in this analysis is a 600 kilometer orbit.

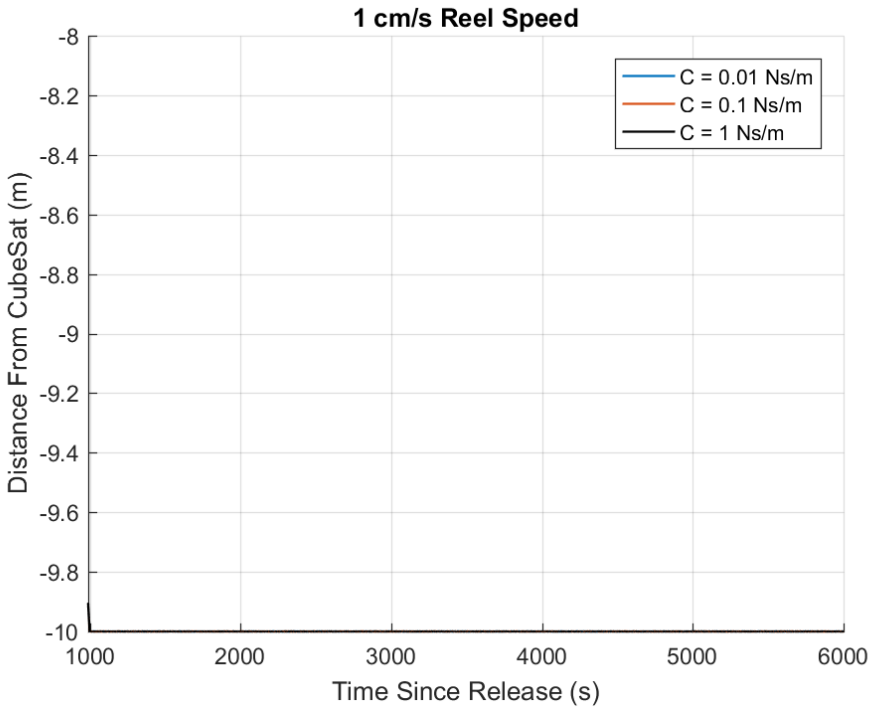

Figure 18: 1 cm/s Tether Release Settling Time at 600 km

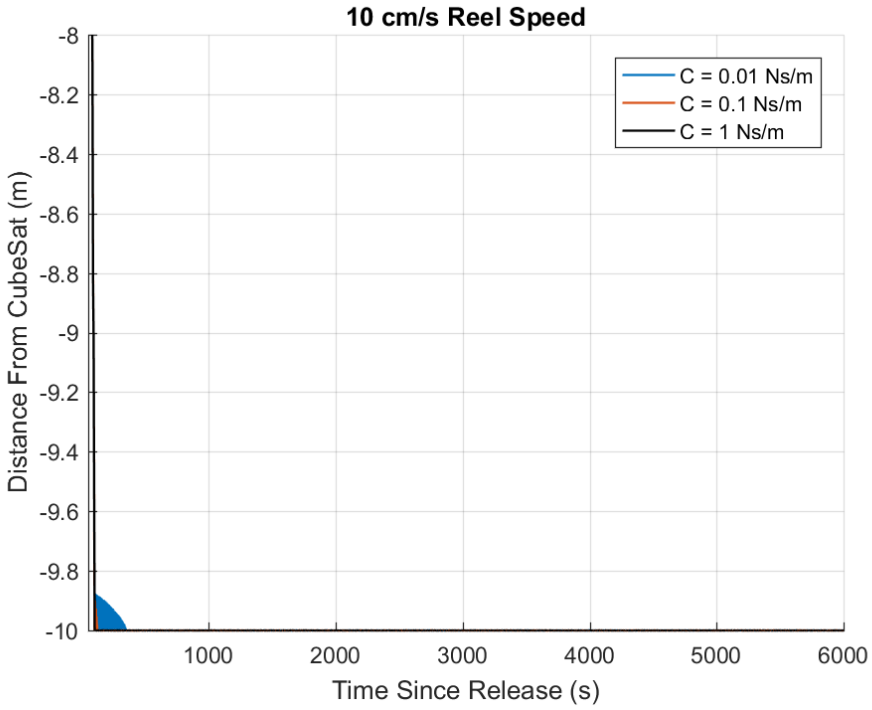

Figure 19: 10 cm/s Tether Release Settling Time at 600 km

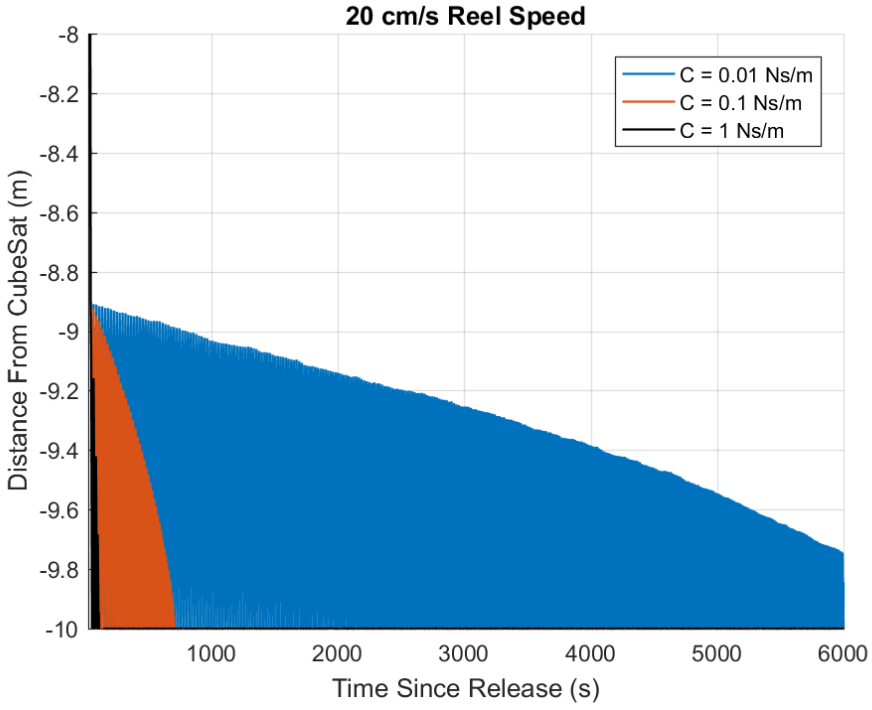

Figure 20: 20 cm/s Tether Release Settling Time at 600 km

The figures above show the importance of being able to control the speed at which the tether is released. The plots show the position of the target with respect to the CubeSat, with the -10 meter mark being at full extension. The figures appear filled in due to the length of time being simulated but the in reality there are oscillations with periods of up to 30 seconds as the tether reaches full extension and rebounds. The amplitude of the oscillations as well as the settling

time for more rapid release speeds are drastically higher than those that are slower. The one centimeter per second speed showed almost no rebounding behavior whatsoever even at the lowest damping coefficient. The longer it takes for the system to settle the higher the risk of the system becoming unstable as it will be uncontrollable when there is any slack present in the tether.

VI. System Requirements

This analysis also aims to define requirements for several of the components being considered for the mission. These requirements are primarily for attitude determination and control system (ADCS) and cover the reaction wheel requirements, pointing requirements, and field of view requirements for the optical camera.

A. Reaction Wheel Requirements

The reaction wheels on board the spacecraft must be able to track the target as it drifts away from the CubeSat. This will occur faster, and thus have more strict requirements, at lower altitudes due to the higher drag. 42 was used to simulate the positions of both bodies at an initial orbit altitude of 300 kilometers to determine the necessary slew rate the spacecraft must be able to achieve to successfully track the target. These rates are plotted below until the time when the separation between the spacecraft and target exceeds 10 kilometers.

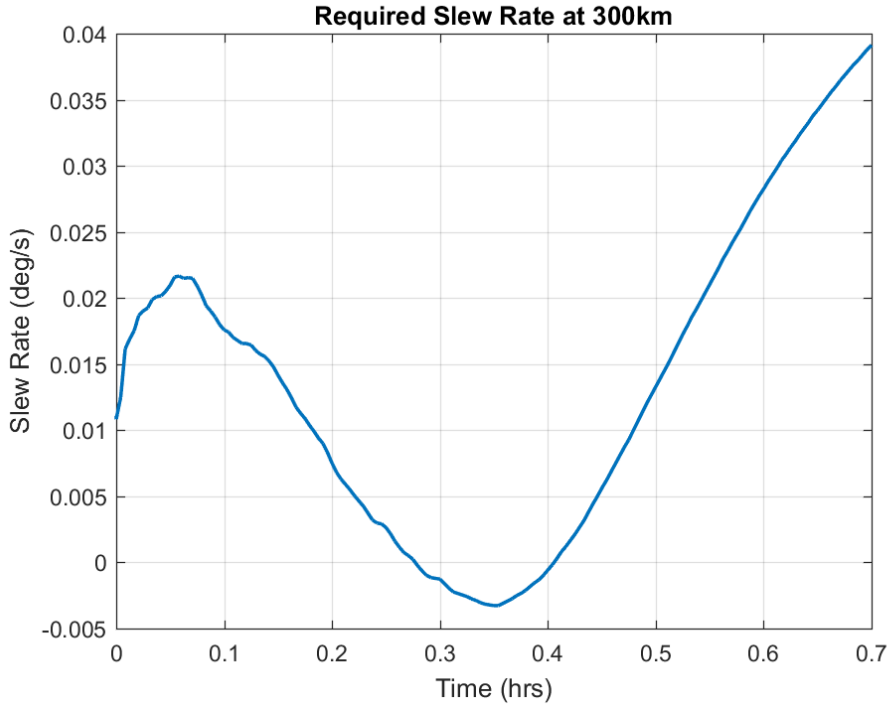

Figure 21: Target Tracking Required Slew Rate at 300km Target Release

The CubeSat must be able to accelerate to 0.022 degrees per second in 180 seconds this is the fastest angular acceleration required during the maneuver. This requires and angular acceleration of $1.22*10^{-4}$ degrees per square second. Given the Inertia properties of the CubeSat this will require a torque of $7.99*10^{-5}$ millinewton meters of torque. To obtain an angular rate of 0.04 degrees per second the reaction wheels will also need to store $2.6 *10^{-2}$ millinewton seconds of momentum. This is well within the capabilities of most reaction wheels.

B. Pointing Requirements

In addition to being able to perform the necessary slew maneuver to track the target the system must also be able to accurately point the spacecraft at the target as it drifts away. To determine the necessary pointing requirements of the system four cases are considered, combining the target being at 5 or 10 kilometers and a 1 milliradian laser and a

0.1 milliradian laser. The apparent size of the target is 41.25 arcseconds at 5 kilometers and 20.62 arcseconds at 10 kilometers. The 1 milliradian laser has an angular size of 206.3 arcseconds and the 1 milliradian laser has a size of 20.63 arcseconds. The following table shows the pointing requirements to ensure the CubeSat is able to keep the laser on target.

Table 4: Minimum System Pointing Requirements

	1 mRad	*0.1 mRad*
5 km	123.78 arcseconds	30.94 arcseconds
10 km	113.46 arcseconds	20.62 arcseconds

These values were calculated as using the sum of half of the angular sizes of the target and laser and represent the absolute minimum pointing requirements to have the target in the field of view of the laser.

C. Optical Camera Field of View Requirements

The optical camera must be able to track the target as it moves so the target must remain within the field of view of the camera. The maximum angle that the target is anticipated to drift from the ram direction at the various altitudes being considered can be seen in Figures 9 through 15. The required field of view of the optical camera is simply twice the amplitude of the greatest oscillations anticipated. These values as a function of altitude can be seen in the following table.

Table 5: Optical Camera FOV Requirements

Altitude (km)	*FOV (deg)*
300	4
350	5
400	16
450	22
500	50
550	110
600	240

VII. Conclusion

The high surface area of the target being deploy in combination with the short length of the tether being used makes the attitude dynamics of the TARGIT mission unique when compared to previously flown tethered space systems. Simulations conducted using both single element and multi-element tethers suggest that an uncontrolled system carries a great risk of developing oscillations that ultimately lead to the system becoming unstable. If this were to occur during the mission the satellite and target risk colliding or becoming entangled by the tether both of which could result in mission failure. Using the CubeSat to actively damp the system shows promise in minimizing the oscillations in the system and maintaining long term stability. The deployment speed of the tether was also examined. The simulation results suggest that a deployment speed of one centimeter per second or less would be ideal to prevent bounce back of the target once it reaches full deployment. This should be possible as the TARGIT mission intends to use a motorized system to deploy the target. Requirements for the attitude determination and control subsystem based on this analysis are well within the capabilities available off the shelf technology.

References

[1] Cosmo, M., Lorenzini, E. (1997), Tethers In Space Handbook Third Edition, Smithsonian Astrophysical Observatory

[2] European Space Agency (2013), The YES Program, retrieved April 04, 2018, from https://www.esa.int/Education/Young_Engineers_Satellites/The_YES_programme

[3] Atsuko Uchida, Masahiro Nohmi, “STARS-II mission design for space experiment of tethered robotic system,” Proceedings of i-SAIRAS (International Symposium on Artificial Intelligence, Robotics and Automation in Space), Turin, Italy, Sept. 4-6, 2012
[4] National Aeronautics and Space Administration (2012), “Earth's Energy Budget Remained Out of Balance Despite Unusually Low Solar Activity”, retrieved April 04, 2018 from https://www.giss.nasa.gov/research/news/20120130b/
[5] Boradway, N. (1971) “Radiation Effects Design Handbook”, National Aeronautics and Space Administration
[6] Curtis, Howard D. “Orbital Mechanics for Engineering Students”. Elsevier, 2014. pp. 631-641
[7] Bell, I, et al (2013), “Investigating Miniature Electrodynamic Tethers and Interaction with the Low Earth Orbit Plasma”, AIAA Space 2013 Conference and Exposition
[8] Bronner, B, Trung, D.(2015) “Developing the Miniature Tether Electrodynamics Experiment”, University of Michigan
[9] Lanoix, E. (1999), “A Mathematical Model for the Long-Term Dynamics of Tethered Spacecraft”, McGill University